Chapter 2

Photoinduced Pseudospin Dynamical Effects in Graphene-Like Systems

Alexander López and Benjamin Santos

Additional information is available at the end of the chapter

http://dx.doi.org/10.5772/67618

Abstract

In this chapter, we describe some of our recent results on the laser-induced manipulation of the energy band structure of graphene-like systems. We present numerical results on the quasi-energy spectrum as well as detailed calculations of semi-analytical approximations to other physical quantities of interest. The main message we would like to convey to the interested reader of the chapter is that by properly tuning the perturbation parameters of the radiation field one can control the size and shape of the photoinduced gaps. These in turn would allow the realization of new electronic phases on graphene and its related materials such as silicene.

Keywords: graphene, light-matter interaction, Floquet theory, Dirac fermions, Landau levels, pseudospin polarization

1. Introduction

Since its recent experimental realization [1], graphene has attracted a lot of research interest because of its remarkable transport properties. At low energy, single-layer graphene (SLG) has a *linear dispersion spectrum*, and charge carriers can be described as massless, chiral, Dirac fermions. Moreover, SLG is a zero-gap semiconductor, has a high mobility of charge carriers and features an unconventional half-integer quantum Hall effect which can be measured at room temperature [2]; therefore, it has been the focus of many experimental [3] and theoretical analyses [4, 5], and it is expected to have several potential applications in carbon-based spintronics. Thus, the study of spin-related transport phenomena is one of the most active research fields in graphene. One important breakthrough was the demonstration of a quantum spin Hall effect in

SLG [6]. This in turn relies on intrinsic spin-orbit coupling (SOC), which although weak compared to other energy scales in the problem [7] opens a gap in the energy spectrum, making SLG into a topological insulator. Another possibility for SOC is due to interactions with a substrate, the presence of electric fields or curvature of the SLG. Therefore, it is called extrinsic or Rashba spin-orbit coupling (RSOC). The RSOC is believed to be responsible for spin polarization [8], and spin relaxation phenomena in graphene [9]. In addition, in the presence of an external magnetic field B, Landau's quantization leads to a $\sqrt{B}$ energy relation which contrasts the linear in B dependence of conventional 2DEG, with parabolic energy bands.

Indeed, one interesting aspect of the new graphene-like materials is that they are predicted to support the so-called edge states which are related to the realization of new topological aspects of matter. As it has been acknowledged in the recent literature, since the discovery of the quantum Hall effect [10, 11], the quest for new topological states of matter has attracted a great deal of attention (for a recent review, see Ref. [12]). For instance, some proposals to topologically generate and characterize non-trivial phases in graphene have paved the road for research on how to implement models of non-trivial topological states in different physical systems ranging from semiconducting quantum wells [13], superconductors [14] and neutral [15] and cold atoms [16], just to mention a few.

In Ref. [13], a model for quantum spin Hall (QSH) state in telluride-based quantum wells was analysed. Yet, it was shown afterwards that this model really corresponds to a topological insulator state [17]. In general, a topological insulator is a quantum state of matter where a given material supports edge states that counter-propagate on its boundary. The existence of these edge states allows for non-dissipative transport, which is a most-wanted property in technological implementations, for instance, in quantum information and nanotechnological devices. In principle, the topological-insulating phase is protected by time-reversal symmetry. However, a time-reversal-symmetry-broken QSH state proposal was recently put forward by means of ferromagnetic leads attached to the sample [18].

Upon introduction of time-periodic dynamical modulation, for instance, in semiconducting quantum wells, with a zincblende structure, it has been recently shown that AC driving can induce a topological phase transition leading to the so-called Floquet topological insulator (FTI) phases [19]. This means that a non-trivial topological phase can be induced in a system that in equilibrium behaves trivially [20–22], that is, it does not possess non-dissipative or gapless edge states.

In this chapter, we show some of our results on the photoinduced effects on the Dirac fermions of graphene-like systems presenting two specific scenarios. In Section 2, we describe the Landau levels (LLs) in graphene when a laser is incident perpendicularly to the sample [23]. We show that an exact effective Floquet Hamiltonian can be found from which the dynamics is afterwards described [24–26]. Here, we show that the quasi-energy spectrum presents a level-dependent photoinduced gap and we also show that coherent Landau level states can be synchronized in order to produce Rabi oscillations and quantum revivals [27]. In Section 3, we describe how the energy spectrum and pseudospin polarization in monolayer silicene [28–33] can be manipulated beyond the so-called off-resonant regime [34, 35] when strong radiation effects are taken into account [36–38]. We find the explicit and realistic parameter regime

for the realization of a single-valley polarized state in silicene. In Section 4, an outlook is given whereas in Section 5 we present some technical details of the calculations employed because although we know there are several works describing the dynamical aspects of periodically driven systems, we wanted to be self-contained. Another reason for delving into such details is that we think this explicit technical aspect could be useful for both students and researchers interested in the field.

2. Technical aspects of periodically driven systems

2.1. Floquet Fourier-mode approach

Before delving into the models of interest, let us present a summary of an important tool in the description of time-dependent Hamiltonian dynamics when the interaction term is periodic in time. These kinds of interactions are ubiquitous in physical systems ranging from cold atoms, cavity QED, superconducting interferometric devices, lasers, and so on. Let us then consider a generic time-dependent periodic Hamiltonian $H(t+T)=H(t)$. We write it as free Hamiltonian plus a time-dependent interaction

$$H(t)=H_0+V(t). \tag{1}$$

The solution of the dynamics for the evolution operator

$$i\hbar\partial_t U(t)=H(t)U(t), \tag{2}$$

is formally given by

$$U(t)=\mathcal{T}\left[\exp\left(-\frac{i}{\hbar}\int_0^t H(t')dt'\right)\right], \tag{3}$$

with $\mathcal{T}$ the time-ordering operator. However, since the Hamiltonian $H(t)$ is periodic, one can resort to Floquet theorem [24, 25]. It asserts that the general solution to the dynamics (2) when $H(t)$ is periodic can be written as

$$U(t)=P(t)e^{-iH_F t/\hbar}, \tag{4}$$

with $P(t)$ periodic and H_F a constant matrix, respectively. Using Eq. (4), it is easy to verify the stroboscopic property

$$U(nT)=P(nT)e^{-inTH_F/\hbar} \tag{5}$$

$$U(nT)=[U(T)]^n, \tag{6}$$

where $U(T)=e^{-iH_F T/\hbar}$. Thus, although the time-dependent Hamiltonian $H(t)$ is periodic, the corresponding evolution operator $U(t)$ is not, that is, $U(t+T)\neq U(t)$. In fact, $U(T)$ carries non-trivial information on the dynamics of the periodic system. The eigenvalues of H_F give the

quasi-energy spectrum of the periodically driven problem. In order to determine these quasi-energies, one standard approach (see below) consists of performing an expansion in the (infinite) eigenbasis of time periodic functions $\xi_n(t) = e^{in\omega t}$ (Fourier modes), where $\omega = 2\pi/T$. Then, in order to deal with the infinite eigenvalue problem one resorts to a truncation procedure in order to determine the Floquet exponents.

In the following, we would like to explicitly describe the Floquet-Fourier mode strategy. For this purpose, we assume that we can solve the dynamics of the free part H_0. Its eigenbasis is spanned by the spinors $|\phi_\alpha\rangle$, where α describes a set of quantum numbers. We now use the eigenstates $|\phi_\alpha\rangle$ as expansion basis for the eigenstates of the full Hamiltonian in Eq. (1).

In order to analyse the evolution equation,

$$i\hbar\partial_t|\Phi(t)\rangle = H(t)|\Phi(t)\rangle \tag{7}$$

we take advantage of the periodicity of the Hamiltonian so we can resort to Floquet's theorem [24, 25]. For this purpose, we define an auxiliary Hermitian Hamiltonian

$$\mathcal{H}(t) = H(t) - i\hbar\partial_t, \tag{8}$$

along with the so-called Floquet states

$$|\Psi_\alpha(t)\rangle = \exp(i\varepsilon_\alpha t/\hbar)|\Phi(t)\rangle \tag{9}$$

such that

$$\mathcal{H}(t)|\Psi_\alpha(t)\rangle = \varepsilon_\alpha|\Psi_\alpha(t)\rangle \tag{10}$$

which are periodic functions of time, $|\Psi_\alpha(t+T)\rangle = |\Psi_\alpha(t)\rangle$. In addition, the eigenvalues ε_α form the quasi-energy spectrum, and are the analogous of the quasi-momenta for Bloch electrons in a spatially periodic structure.

We can verify that the states

$$|\Psi_{\alpha n}(t)|\rangle = \exp(in\omega t)|\Psi_\alpha(t)\rangle \tag{11}$$

are also eigenstates of the Hamiltonian $\mathcal{H}(t)$ but with corresponding eigenvalues $\varepsilon_\alpha \to \varepsilon_\alpha + n\hbar\omega$. Thus, we can work in the *first Brillouin zone* $-\hbar\omega/2 \le \varepsilon_\alpha \le \hbar\omega/2$.

Using the periodic temporal basis $\xi_n(t) = \exp(in\omega t)$, which satisfies

$$\frac{1}{T}\int_0^T \xi_n^*(t)\xi_m(t) = \delta_{nm}, \tag{12}$$

we write the Fourier-mode expansion

$$\Phi_\alpha(t) = \exp(-i\varepsilon_\alpha t)\sum_{n=-\infty}^{n=\infty}|C_\alpha^{(n)}\rangle\xi_n(t), \tag{13}$$

Now, we use the expansion $|C_\alpha^{(n)}\rangle = \sum_\beta \Lambda_{\alpha\beta}^{(n)}|\phi_\beta\rangle$ such that Eq. (10) becomes

http://dx.doi.org/10.5772/67618

$$H(t)\sum_{n=-\infty}^{n=\infty}\sum_{\beta}\Lambda_{\alpha\beta}^{(n)}|\phi_\beta\rangle\xi_n(t)+$$
$$\sum_{n=-\infty}^{n=\infty}\sum_{\beta}\Lambda_{\alpha\beta}^{(n)}|\phi_\beta\rangle\xi_n(t)(\varepsilon_\alpha-n\hbar\omega)=0. \tag{14}$$

Multiplication by $\langle\phi_\gamma|\xi_m^*(t)$, then average over one temporal period, leads to

$$\sum_{n=-\infty}^{n=\infty}\sum_{\beta}[\langle\alpha|H^{(m-n)}|\beta\rangle-(\varepsilon_\alpha-n\hbar\omega)\delta_{nm}\delta_{\alpha\beta}]\Lambda_{\alpha\beta}^{(n)}=0. \tag{15}$$

and we have used the simplifying notation $|\alpha\rangle\equiv|\phi_\alpha\rangle$, and $H^{(m-n)}=1/T\int_0^T\xi_m^*(t)H(t)\xi_n(t)$.

Then, the quasi-energies ε_α are eigenvalues of the secular equation.

$$det|H_F-\varepsilon_\alpha|=0 \tag{16}$$

where $\langle\langle\alpha m|H_F|n\beta\rangle\rangle=H_{\alpha\beta}^{(m-n)}+m\omega\delta_{nm}\delta_{\alpha\beta}$. Here, we simplify the notation to represent the direct product of orbital and periodic eigenfunctions $|\alpha m\rangle\rangle\equiv|\alpha\rangle\otimes\xi(t)$.

For example, for a two-level problem we could take the interaction in the form $V(t)\propto\vec{\sigma}\cdot\vec{A}(t)$. Then, if the vector potential given as $\vec{A}(t)=A(\cos\omega t,\sin\omega t)$, we find that H^{m-n} has non-vanishing elements only for $m-n=0,\pm1$ as it is described in the following section.

2.2. Off-resonant approximation

In some physical scenarios, the frequency of the radiation field is way much larger than any other energy scale in the problem. Within this regime, one can derive an approximate Floquet Hamiltonian that captures the essence of the photoninduced bandgaps. In order to describe this so-called off-resonant regime, let us begin by explicitly showing the effective Floquet Hamiltonian: For this purpose, let us start from the general periodic Floquet Hamiltonian given in Eq. (1)

$$H(t)=H_0+V(t), \tag{17}$$

where H_0 is the static contribution and $V(t+T)=V(t)$ is the time-periodic interaction. Going to Fourier space, we get the general structure of the Floquet Hamiltonian in matrix form as

$$\begin{pmatrix}
\ddots & & & & & & & \\
\cdots & V_{-2,-3} & H_0-2\Omega & V_{-2,-1} & V_{-2,0} & V_{-2,1} & V_{-2,2} & \cdots \\
\cdots & V_{-1,-3} & V_{-1,-2} & H_0-\Omega & V_{-1,0} & V_{-1,1} & V_{-1,2} & \cdots \\
\cdots & V_{0,-3} & V_{0,-2} & V_{0,-1} & H_0 & V_{0,1} & V_{0,2} & \cdots \\
\cdots & V_{1,-3} & V_{1,-2} & V_{1,-1} & V_{1,0} & H_0+\Omega & V_{1,2} & \cdots \\
 & \vdots & \vdots & \vdots & V_{2,0} & V_{2,1} & H_0+2\Omega & \cdots \\
 & & & & & & & \ddots
\end{pmatrix}, \tag{18}$$

where the interaction submatrices are defined as

$$V_{nn'} = \frac{1}{T}\int_0^T dt V(t) e^{-i(n-n')\Omega t}. \tag{19}$$

For a monochromatic harmonic perturbation, this reduces to a block-tridiagonal matrix

$$\begin{pmatrix} \ddots & & & & & & & \\ \cdots & V_{-1} & H_{-2} & V_{+1} & 0 & 0 & 0 & \cdots \\ \cdots & 0 & V_{-1} & H_{-1} & V_{+1} & 0 & 0 & \cdots \\ \cdots & 0 & 0 & V_{-1} & H_0 & V_{+1} & 0 & \cdots \\ \cdots & 0 & 0 & 0 & V_{-1} & H_1 & V_{+1} & \cdots \\ & \vdots & \vdots & \vdots & 0 & V_{-1} & H_2 & \cdots \\ & & & & & & & \ddots \end{pmatrix}, \tag{20}$$

and to simplify the notation we have set $V_N = V_{n-m}$ and $H_j = H_0 + j\Omega$. If we set out the eigenstate for a given number of Fourier modes n, we will have

$$\Phi = \begin{pmatrix} \phi_{-n} \\ \phi_{-n+1} \\ \vdots \\ \phi_{-2} \\ \phi_{-1} \\ \phi_0 \\ \phi_1 \\ \phi_2 \\ \vdots \\ \phi_{n-1} \\ \phi_n \end{pmatrix}, \tag{21}$$

with each ϕ_n a vector of dimensionality determined by H_0. For instance, if we approximate the problem in such a way that we only consider one Fourier mode ($n = 1$), we have to solve the following system of coupled equations:

$$\begin{aligned} H_{-1}\phi_{-1} + V_{+1}\phi_0 &= E\phi_{-1} \\ V_{-1}\phi_{-1} + H_0\phi_0 + V_{+1}\phi_{+1} &= E\phi_0 \\ H_{+1}\phi_{+1} + V_{-1}\phi_0 &= E\phi_{+1}. \end{aligned} \tag{22}$$

From the first and last equations, we get

$$\begin{aligned} \phi_{-1} &= (E - H_{-1})^{-1} V_{+1}\phi_0 \\ \phi_{+1} &= (E - H_{+1})^{-1} V_{-1}\phi_0, \end{aligned} \tag{23}$$

such that we get an effective equation for ϕ_0

$$[V_{-1}(E - H_{-1})^{-1}V_{+1} + H_0 + V_{+1}(E - H_{+1})^{-1}V_{-1}]\phi_0 = E\phi_0 \tag{24}$$

which explicitly reads

$$[V_{-1}(E - H_0 + \Omega)^{-1}V_{+1} + H_0 + V_{+1}(E - H_0 - \Omega)^{-1}V_{-1}]\phi_0 = E\phi_0 \tag{25}$$

For $\Omega \gg ||H_0||$, that is, frequencies much larger than the typical energy scales of the static problem, we can approximate this as

$$\left(H_0 + \frac{V_{-1}V_{+1}}{\Omega} - \frac{V_{+1}V_{-1}}{\Omega}\right)\phi_0 \approx E\phi_0, \tag{26}$$

so we get the effective approximate Floquet Hamiltonian, valid for large frequencies

$$H_{\mathrm{F}} \approx H_0 + \frac{[V_{-1}, V_{+1}]}{\Omega}. \tag{27}$$

With a similar procedure, one can show that for $n = 2$ one gets the approximate Floquet Hamiltonian

$$H_{\mathrm{F}} \approx H_0 + \frac{[V_{-1}, V_{+1}]}{\Omega} - \frac{1}{2\Omega}\frac{[V_{-1}^2, V_{+1}^2]}{\Omega^2}. \tag{28}$$

These results essentially imply that a photoinduced energy bandgap can be induced by means of the dressed Floquet states that emerge from the off-resonant condition. Needless to say that sometimes the photoinduced energy bandgaps can be tiny; yet, in some circumstances one only needs to make sure that there is a gap, however, small and the topological properties of the driven system can be qualitatively different as those of the undriven (gapless) system.

3. Photoinduced effects of Landau levels

In this section, we summarize our results reported in Ref. [23] where we theoretically analyse the dynamical manipulation of the LL structure of charge carriers on suspended monolayer graphene when a periodically driving radiation field is applied perpendicular to the sample. For this purpose, we focus on the low-energy properties of non-interacting spinless charge carriers in a suspended monolayer graphene subject to a perpendicular, uniform and constant magnetic field $\mathbf{B} = B\hat{z}$. The dynamics is governed by Dirac's Hamiltonian. In coordinate representation, it reads

$$\mathcal{H}_\eta(\mathbf{r}) = v_F(\eta\pi_x\sigma_x + \pi_y\sigma_y), \tag{29}$$

where $v_F \sim 10^6 m/s$ is the Fermi velocity in graphene. In addition, the canonical momenta $\pi_j = p_j + eA_j$ $(j = x, y)$ contain the vector potential ($\nabla \times \mathbf{A} = \mathbf{B}$), $-e$ is the electronic charge ($e > 0$), and $\eta = \pm 1$ describes the valley degree of freedom. Using the definition of the magnetic length $l_B^{-2} = eB/\hbar$ and the cyclotron energy $\hbar\omega_c = \sqrt{2}v_F\hbar/l_B$, the Hamiltonian Eq. (29) at each K (K′) Dirac point, which corresponds to $\eta = +1$ ($\eta = -1$), can be written in the form

$$H_{+1} = \hbar\omega_c \begin{pmatrix} 0 & a \\ a^\dagger & 0 \end{pmatrix} \tag{30}$$

$$H_{-1} = -\hbar\omega_c \begin{pmatrix} 0 & a^\dagger \\ a & 0 \end{pmatrix} \tag{31}$$

where the annihilation and creation operators are defined by standard relations as

$$a = \frac{l_B(\pi_x - i\pi_y)}{\sqrt{2}} \quad \text{and} \quad a^\dagger = \frac{l_B(\pi_x + i\pi_y)}{\sqrt{2}}. \tag{32}$$

The eigenenergies of the Hamiltonian (29) are then

$$E_n^{s,\eta} = s\eta\sqrt{n}\hbar\omega_c \tag{33}$$

with $s = \pm 1$. Positive (negative) values of $s\eta$ represents the conduction (valence) band at each Dirac point. In addition, the integer quantum number $n = 0, 1, 2\ldots$ labels the Landau-level structure of monolayer graphene. Using the eigenstates $|n\rangle$ of the operator $a^\dagger a$, the corresponding eigenstates $|\varphi_n^{s,\eta}\rangle$ read

$$|\varphi_n^{s,+1}\rangle = \frac{1}{\sqrt{2}} \begin{pmatrix} s|n-1\rangle \\ |n\rangle \end{pmatrix} \tag{34}$$

$$|\varphi_n^{s,-1}\rangle = \frac{1}{\sqrt{2}} \begin{pmatrix} -s|n\rangle \\ |n-1\rangle \end{pmatrix} \tag{35}$$

for $n \neq 0$. The zero-energy eigenstate ($n = 0$) is given in each case by

$$|\varphi_0^{+1}\rangle = \begin{pmatrix} 0 \\ |0\rangle \end{pmatrix} \tag{36}$$

$$|\varphi_0^{-1}\rangle = \begin{pmatrix} |0\rangle \\ 0 \end{pmatrix}. \tag{37}$$

Due to time-reversal symmetry, we have $\mathcal{T}H_{+1}\mathcal{T} = H_{-1}$. Let us now consider the effect of intense circularly polarized terahertz electromagnetic radiation, incident perpendicularly to the sample. We assume that the beam radiation spot is large enough compared to the lattice spacing so we can neglect any spatial variation. According to the standard light-matter interaction formulation, the dynamical effects of a monochromatic radiation field incident perpendicular to the sample can be described by means of a time-dependent vector potential

$$\mathbf{A}(t) = \frac{\mathcal{E}}{\omega}(\cos\omega t, \delta \sin\omega t), \tag{38}$$

where $\boldsymbol{\mathcal{E}}$ and ω are, respectively, the amplitude and frequency of the electric field given in turn by the standard relation $\boldsymbol{\mathcal{E}}(t) = -\partial_t \mathbf{A}(t)$. In addition, we are using $\delta = +1$ ($\delta = -1$) for right (left) circular polarization. We are using circular polarization because it has been shown to

provide the maximal photoinduced bandgap. Starting from the ordinary dipolar interaction term $-e\mathbf{p}\cdot\mathbf{A}(t)$, introduced to the tight-binding Hamiltonian via the Peierls substitution, we can evaluate the effects of the driving at each Dirac point as

$$V_\eta = ev_F[\eta\sigma_x A_x(t) + \delta\sigma_y A_y(t)], \tag{39}$$

which explicitly reads

$$V_\eta = \xi\eta(\sigma_x \cos\omega t + \eta\delta\sigma_y \sin\omega t). \tag{40}$$

with the effective coupling constant $\xi = ev_F\mathcal{E}/\omega$. This makes the total Hamiltonian

$$H_\eta(t) = H_\eta + V_\eta(t), \tag{41}$$

periodic in time $H_\eta(t+T) = H_\eta(t)$, with $T = 2\pi/\omega$ the period of oscillation of the driving field. Therefore, if we focus on the K Dirac point ($\eta = 1$), the physics at the K′ Dirac point ($\eta = -1$) can be easily found by the substitutions $\xi \to -\xi$ and $\omega \to -\omega$.

Thus, let us focus on the K point physics and afterwards, we can make the necessary substitutions. In order to simplify the notation, we set $H_{+1} = H_0$ and $V_{+1}(t) = V(t)$. Hence, defining rising σ_+ and lowering σ_- pseudospin operators by the standard formulas

$$\sigma_\pm = \frac{\sigma_x \pm i\sigma_y}{2}, \tag{42}$$

the time-dependent interaction potential can be rewritten as

$$V(t) = \xi(e^{-i\delta\omega t}\sigma_+ + e^{i\delta\omega t}\sigma_-), \tag{43}$$

Now, we invoke Floquet's theorem which states that the time evolution operator of the system induced by a periodic Hamiltonian can be written in the form [24]

$$U(t) = P(t)e^{-iH_F t/\hbar}, \tag{44}$$

with $P(t)$ a periodic unitary matrix and H_F a time-independent dynamical generator referred to as the Floquet Hamiltonian. The eigenvalues of the Floquet Hamiltonian H_F represent the quasi-energy spectrum of the periodically driven system. Typically, in order to solve for the quasi-energy spectrum, one can expand each term of the time-dependent Schrödinger equation in Fourier space and numerically solve an infinite eigenvalue problem. Instead, we will take a perturbative approach as discussed below.

Accordingly, for our problem we can find approximate solutions to the dynamics by modifying slightly the analytical strategy presented in Ref. [39]. Then, one finds that the excitation number operator, N_a, defined as

$$N_a = \left(a^\dagger a + \frac{1}{2}\right)\mathbb{1} + \frac{\sigma_z}{2}, \tag{45}$$

which commutes with the Hamiltonian H_0 and satisfies the eigenvalue equation

$$N_a|\varphi_n^s\rangle = n|\varphi_n^s\rangle. \tag{46}$$

N_a generates a time-dependent unitary transformation $|\Psi(t)\rangle = P(t)|\Phi(t)\rangle$ given as

$$P(t) = \exp(-iN_a\delta\omega t), \tag{47}$$

such that the time-dependent Schrödinger equation

$$i\hbar\partial_t|\Psi(t)\rangle = H(t)|\Psi(t)\rangle \tag{48}$$

can be transformed with a time-independent operator H_F governing the dynamics of the problem

$$i\hbar\partial_t|\Phi(t)\rangle = H_F|\Phi(t)\rangle, \tag{49}$$

where H_F and $|\Phi(t)\rangle$ are the Floquet Hamiltonian and Floquet eigenstate, respectively. Conducting the explicit calculation, H_F is found to be given by

$$H_F = H_0 - N_a\delta\hbar\omega + \xi\sigma_x, \tag{50}$$

where the effective coupling to the radiation field is $\xi = ev_F\mathcal{E}/\omega$. This Hamiltonian can be treated via non-degenerate perturbation theory to find the approximate quasi-energy spectrum (see Ref. [23] for details on the derivation), which read

$$\epsilon_m^s = s\sqrt{m(\hbar\omega_c)^2 + (m\xi)^2}, \text{mod}\hbar\omega. \tag{51}$$

The associated mean energies are in turn found as

$$\overline{\epsilon}_m^s = \epsilon_m^s - \omega\frac{\partial\varepsilon_m^s}{\partial\omega}, \tag{52}$$

which are invariant under $\epsilon_m^s \to \epsilon_m^s + l\hbar\omega$, for l being an integer. Conducting the explicit calculation, the mean energies are found to be given by the expression

$$\overline{\epsilon}_m^s = s\left(\frac{m(\hbar\omega_c)^2 + 2m^2\xi^2}{\sqrt{m(\hbar\omega_c)^2 + m^2\xi^2}}\right). \tag{53}$$

As can be seen in **Figure 1**, these mean energies are plotted as function of the quantizing magnetic field B, for different values of the Landau-level index changing the effective coupling ξ. We notice that, at intermediate light-coupling strength, the energy resolution of these levels becomes much better and could experimentally be tested for not so large

http://dx.doi.org/10.5772/67618

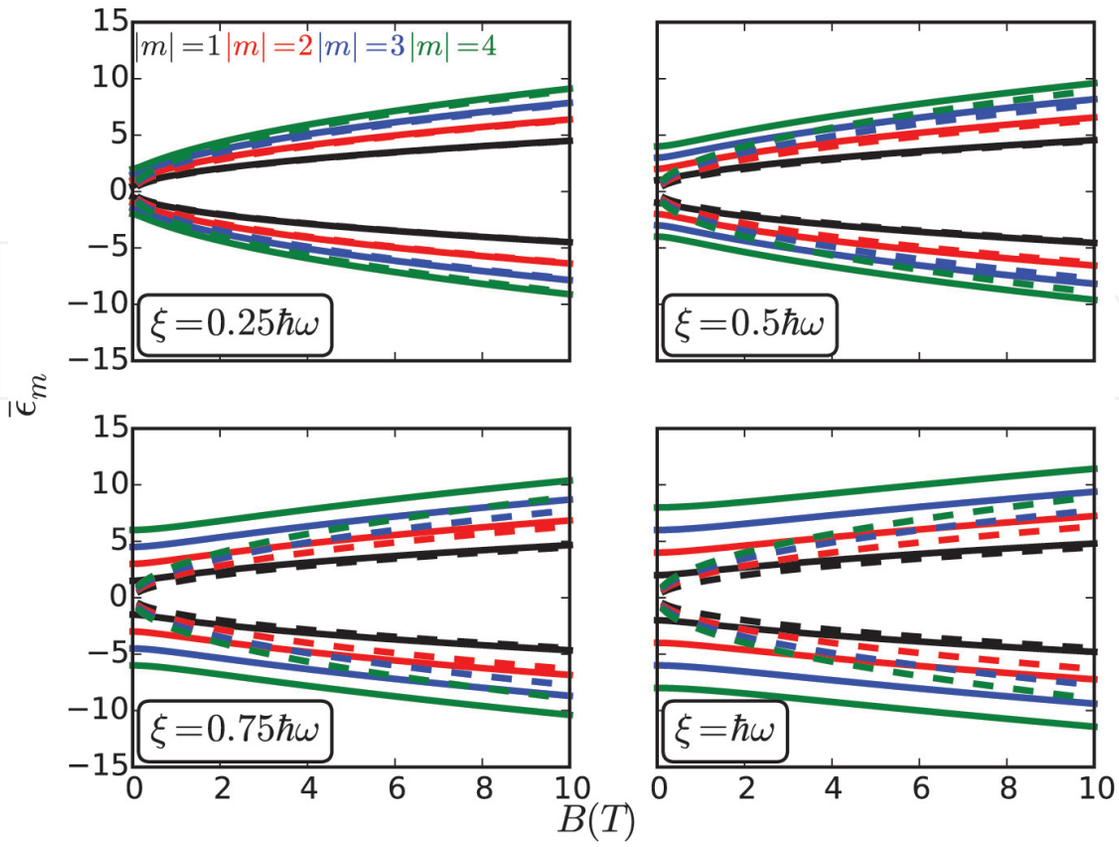

Figure 1. Approximate mean energies for the driven scenario (continuous lines) as function of the quantizing magnetic field B. The dotted lines represent the undriven spectra for the corresponding LL. We notice a level-dependent energy gapped that leads to non-trivial behaviour of physical quantities, as discussed below (see main text). Adapted from Ref. [23] with permission from APS.

quantizing magnetic fields B. Moreover, we find that to this order of approximation the LL becomes gapped, with the striking feature that the photoinduced gap is level-dependent. These gap openings appear except for the $m = 0$ level which, as discussed before, remains insensitive to the radiation field.

3.1. Discussion

So far, we have shown that upon introduction of a perpendicularly radiation field in the Terahertz frequency domain, the Landau-level-quantized scenario can be turned into a level-dependent-gapped system. As shown in reference, this energy bandgap effects can be traced via the oscillations of the pseudospin polarization as well as the temporal evolution of the autocorrelation function for an initially prepared coherent superposition of the static Landau-level configuration. Thus, due to the natural connection between coherent-state superpositions and applications in quantum optics, one could expect that the experimental consequences of such radiation effects on the Landau-level structure of graphene would have some applications within experimentally accessible parameter regimes in the quantum optics realm.

4. Irradiated silicene

As expected, the family of new two-dimensional materials with graphene-like properties has grown in the recent years. However, we show in this section that, although similar in lattice structure, both materials can be experimentally found to have different physical properties. In this section, we focus our attention on silicene which consists of a two-dimensional honeycomb lattice structure of silicon atoms analogous to that of graphene. Some works have reported the synthesis of silicene [30–32]. Silicene has a corrugated or buckled lattice structure that makes the silicon atoms in one sublattice to be perpendicularly displaced with respect to the other sublattice. For this reason, when a perpendicular electric field E_z is applied to silicene, the atoms belonging to each sublattice respond differently to E_z, giving rise to a staggered potential. Due to this peculiar pseudospin response to applied electric fields, and despite their similarities, the electronic properties of silicene are predicted to considerably differ from those of graphene.

In particular, since its intrinsic spin-orbit coupling is much larger than that of pristine graphene, an interesting interplay among intrinsic spin-orbit and electric field effects was predicted to appear because the bandgap can be electrically controlled. Moreover, the addition of an exchange potential term (which physically could represent the proximity effect due to coupling of ferromagnetic leads) allows for topological quantum phase transitions in the static regime [33]. Furthermore, in the presence of circularly polarized electromagnetic radiation, the realization of the so-called single Dirac cone phase in silicene has been recently proposed. At this topological phase, it is found that well-defined spin-polarized states are supported at every Dirac point. Moreover, within this configuration different spin components propagate in opposite directions giving rise to a pure spin current [34]. Yet, these photoinduced topological phase changes [20, 21] reported by Ezawa [34] were derived under the off-resonant assumption, that is, dynamical processes such that the frequency (coupling strength) of the radiation field is much larger (smaller) than any other energy scale in the problem. Under these assumptions, it is possible to derive an effective time-independent Floquet Hamiltonian [24, 25] with a tiny photoinduced bandgap correction that stems from virtual photon absorption and emission processes. Since the sign of the bandgap term (i.e., the effective bandgap) determines important topological properties of the material, it is vital both for potential practical implementations, for instance, in technological realizations of silicene-based devices, and from a fundamental point of view, to effectively achieve manipulation of this quantity.

In this section, we show via an exactly solvable model, where in order to detect physically relevant photoinduced effects in the energy band structure of silicene under strong circularly polarized electromagnetic radiation in the terahertz (frequency) domain one needs to go beyond the aforementioned off-resonant approximation. Indeed, we find that a zero momentum, the obtained exactly solvable time-dependent Hamiltonian, suggests the range of control parameters that physically might lead to experimentally feasible realization of new topological phases in silicene.

4.1. Model

Let us consider the Dirac cone approximation to describe the dynamics of non-interacting charge carriers in silicene subject to a perpendicular, uniform and constant electric field

$\mathbf{E} = E_z\hat{z}$. This is given by the 8×8 Hamiltonian [33] ($\hbar = e = 1$, with e being the electron's charge)

$$\begin{aligned}\mathcal{H}^{\eta} = v_F(k_x\sigma_x + \eta k_y\sigma_y) + \sigma_z(\eta s_z\lambda_{so} - lE_z)\\ +\eta\sigma_z h_{11} + h_{22}\end{aligned} \tag{54}$$

where $v_F = \frac{\sqrt{3}at_b}{2} \approx 8.1\times10^5$ m/s is the Fermi velocity for charge carriers in silicene, with $a = 3.86$ Å the lattice constant and $t_b = 1.6$ eV the hopping parameter within a tight-binding formulation, whereas $l = 0.23$ Å measures half the separation among the two sublattice planes. In addition, $\eta = \pm1$ describes the Dirac point, σ_i and s_i ($i = x, y, z$) are Pauli matrices describing pseudo- and real-spin degrees of freedom, respectively, whereas $\vec{k} = (k_x, \eta k_y)$ is the momentum measured from the Dirac point $\eta = \pm1$. The parameter $\lambda_{so} = 3.9$ meV represents the strength of the intrinsic spin-orbit contribution. Moreover, the two contributions given by the terms

$$h_{11} = a\lambda_{R2}(k_y s_x - k_x s_y), \tag{55}$$

$$h_{22} = \lambda_{R1}(\eta\sigma_x s_y - \sigma_y s_x)/2, \tag{56}$$

describe the spin-orbit coupling associated to the next nearest neighbour hopping and nearest neighbour tight-binding formulation, respectively.

The term h_{11} has its origin in the buckled structure of silicone, whereas h_{22} is induced by the application of an external static electric field E_z. Using first-principle calculations, the authors of Ref. [40] found that $\lambda_{R2} = 0.7$ meV and typically h_{22} are of order μeV and thus much smaller than the other energy scales in the problem. Therefore, these two non-conserving contributions will be neglected in the following, although in the appendix we show that the largest contribution h_{11} can be easily incorporated in the solution to the dynamical evolution presented below. Yet, we have verified that our results do not qualitatively change by the introduction of these two small corrections.

Within the approximation $h_{22} = 0$, let us now consider the pseudospin dynamics under an *intense* radiation field represented by the time-dependent vector potential

$$\mathbf{A}(t) = A(\cos\Omega t, \sin\Omega t), \tag{57}$$

with $A = \mathcal{E}/\Omega$ and Ω its amplitude and frequency, respectively. It describes a monochromatic electromagnetic wave incident perpendicular to the sample. This vector potential can in turn be derived from the corresponding electric field by means of $\mathbf{E}(t) = -\partial_t\mathbf{A}(t)$, where $\mathcal{E}$ is the amplitude of the time-dependent electric field.

Using the standard minimal coupling prescription given as $\vec{k} \to \vec{k} + \vec{A}$, we get the dynamical generator

$$\begin{aligned}\mathcal{H}^{\eta}(\vec{k},t) = v_F(k_x\sigma_x + \eta k_y\sigma_y) + \sigma_z(\eta s_z\lambda_{so} - lE_z)\\ v_F A[e^{i\eta\Omega t}\sigma_- + e^{-i\eta\Omega t}\sigma_+].\end{aligned} \tag{58}$$

In the following, we explore the emerging photoinduced dynamical features at zero momentum since this scenario allows for an exact analytical solution to the dynamical evolution equations. Given the fact that we have an exact analytical solution, we can explore the low-, intermediate-, and strong-coupling regimes of the charge carriers in silicene under the radiation field. We then discuss this exact solution and argue the need to explore either the intermediate or strong light-matter-coupling regimes in order to obtain experimentally observable modifications in the physical properties of the system within the irradiation configuration.

4.2. Physics at $k = 0$

In this subsection, we explicitly analyse another exactly solvable model for a graphene-like system. Let us then focus on the zero-momentum scenario for which the extrinsic spin-orbit term h_{11} vanishes and the z-component of spin $s_z = \pm 1$ is a good quantum number. Therefore, the following analysis is independent of taking into account the aforementioned spin-orbit contribution. Setting for notational convenience $\alpha = v_F A$ and $V_z = lE_z$, the physics at zero momentum $\vec{k} = 0$ is described by the dynamical generator

$$\mathcal{H}^{\eta}(0,t) = (\eta s \lambda_{so} - V_z)\sigma_z + \alpha[e^{i\eta\Omega t}\sigma_- + e^{-i\eta\Omega t}\sigma_+]. \tag{59}$$

Using the unitary transformation

$$\mathcal{P}^{\eta}(t) = e^{-i\eta(\mathbb{1}+\sigma_z)\Omega t/2} \tag{60}$$

we get the effective time-independent Floquet Hamiltonian $\mathcal{H}_F(k=0) = (\mathcal{P}^{\eta})^{\dagger}(t)\mathcal{H}^{\eta}(0,t)\mathcal{P}^{\eta}(t) - i(\mathcal{P}^{\dagger})^{\eta}(t)\dot{\mathcal{P}}^{\eta}(t)$

$$\mathcal{H}_F(k=0) = -\frac{\eta\Omega}{2}\mathbb{1} + \left[\eta\left(s_z\lambda_{so} - \frac{\Omega}{2}\right) - V_z\right]\sigma_z + \alpha\sigma_x. \tag{61}$$

Thus, the zero-momentum quasi-energy spectrum is given as

$$\varepsilon^{\eta}_{s\sigma}(k=0) = -\frac{\eta\Omega}{2} + \sigma\sqrt{\alpha^2 + (\Delta^{\eta}_s)^2}, \tag{62}$$

where $s, \sigma = \pm 1$ represent the real- and pseudospin degrees of freedom, respectively. In addition, we have defined the effective gap

$$\Delta^{\eta}_s = \eta\left(s\lambda_{so} - \frac{\Omega}{2}\right) - V_z. \tag{63}$$

On the other hand, the zero-momentum exact Floquet eigenstates are

$$|\psi^{\eta}_{s\sigma}(t)\rangle = \frac{e^{-i\varepsilon^{\eta}_{s\sigma}t}}{\sqrt{2\Gamma}}\begin{pmatrix} e^{-i\eta\Omega t}\sqrt{\Gamma + \sigma\Delta^{\eta}_s} \\ \sigma\sqrt{\Gamma - \sigma\Delta^{\eta}_s}\end{pmatrix}, \tag{64}$$

with $\Gamma = \sqrt{\alpha^2 + (\Delta^{\eta}_s)^2}$.

Some comments are in order at this point. The exact quasi-energy spectrum resembles the solution for the Rabi problem and one could expect that Rabi oscillations should appear in the dynamical evolution of this zero-momentum solution. Moreover, since we are interested in analysing the behaviour of a topological quantity not in terms of the momentum variable but assuming as a toy model that one explores the V_z parameter space along with the 'torus' for the time domain $0 \leq t \leq T$, one could evaluate the components of the pseudospin operator $\hat{\vec{S}}_\alpha$ defined within each subband as

$$\hat{\vec{S}}^{\eta} = \langle \psi^{\eta}_{s\sigma}(t) | \vec{s} | \psi^{\eta}_{s\sigma}(t) \rangle \tag{65}$$

After some algebra, we get

$$\hat{\vec{S}}^{\eta} = \eta(-\sin\beta \sin\Omega t, \sin\beta \cos\Omega t, -\cos\beta) \tag{66}$$

where

$$\tan\beta = \frac{2\alpha}{|\Delta^{\eta}_s|}. \tag{67}$$

Thus, within this limit, the average out-of-plane pseudospin polarization $\overline{S}^z_\eta$ is the only finite component and it reads

$$\overline{S}^z_\eta = -\frac{\eta|\Delta^{\eta}_s|}{\Gamma} \tag{68}$$

Thus, the main advantage of finding semi-analytical solutions to the dynamical evolution is that closed expressions for the physical quantities of interest can be found in such a way that one can provide further insight into the nature of the physical mechanisms involved and how their interplay leads to a given behaviour of the polarization, charge current and so on.

Let us now assume that the system is initially prepared in the arbitrary state

$$|\Phi(0)\rangle = \begin{pmatrix} \cos\frac{\theta}{2} e^{i\phi/2} \\ \sin\frac{\theta}{2} e^{-i\phi/2} \end{pmatrix}, \tag{69}$$

with $0 \leq \theta \leq \pi$ and $0 < \phi \leq 2\pi$ being spherical coordinates over the Bloch sphere. Thus, the evolution of the pseudospin polarization is given by the standard relation $\sigma_z(t) = \langle \Phi(0)|U^{\dagger}_F(t)\ \sigma_z U_F(t)|\Phi(0)\rangle$, with $U_F(t)$ being the unitary Floquet evolution operator $U_F(t) = \mathcal{P}^{\eta}(t)e^{-i\mathcal{H}_F t}$ (note that σ_z and $\mathcal{P}^{\eta}(t)$ commute with each other). The initial polarization in the state (65) is given by $\sigma_z(0) = \cos\theta$. After some algebra, we find

$$\sigma_z(t) = \frac{2\alpha}{\Gamma} \sin\theta \sin\Gamma t \left(\frac{\Delta^{\eta}_s}{\Gamma} \sin\Gamma t \cos\phi - \cos\Gamma t \sin\phi \right) + \cos\theta \left(1 - \frac{2\alpha^2}{\Gamma^2} \sin^2 \Gamma t \right). \tag{70}$$

In addition, the one-period mean-value pseudospin polarization

$$\langle \sigma_z \rangle = \frac{1}{T}\int_0^T \sigma_z(t)dt, \tag{71}$$

with $T = 2\pi/\Omega$ being the period of oscillations of the driving field, gives then

$$\begin{aligned}\langle \sigma_z \rangle = \alpha \sin\theta \left[\frac{\Delta_s^\eta}{\Gamma^2}\cos\phi(1-\mathrm{sinc}(2\Gamma T)) - T\sin\phi\,\mathrm{sinc}^2(\Gamma T)\right] \\ + \cos\theta\left[1-\frac{\alpha^2}{\Gamma^2}(1-\mathrm{sinc}(2\Gamma T))\right],\end{aligned} \tag{72}$$

where $\mathrm{sinc}(x) = \frac{\sin(x)}{x}$.

In particular, for initial states that have zero polarization ($\theta = \pi/2$), we get the simplified expressions

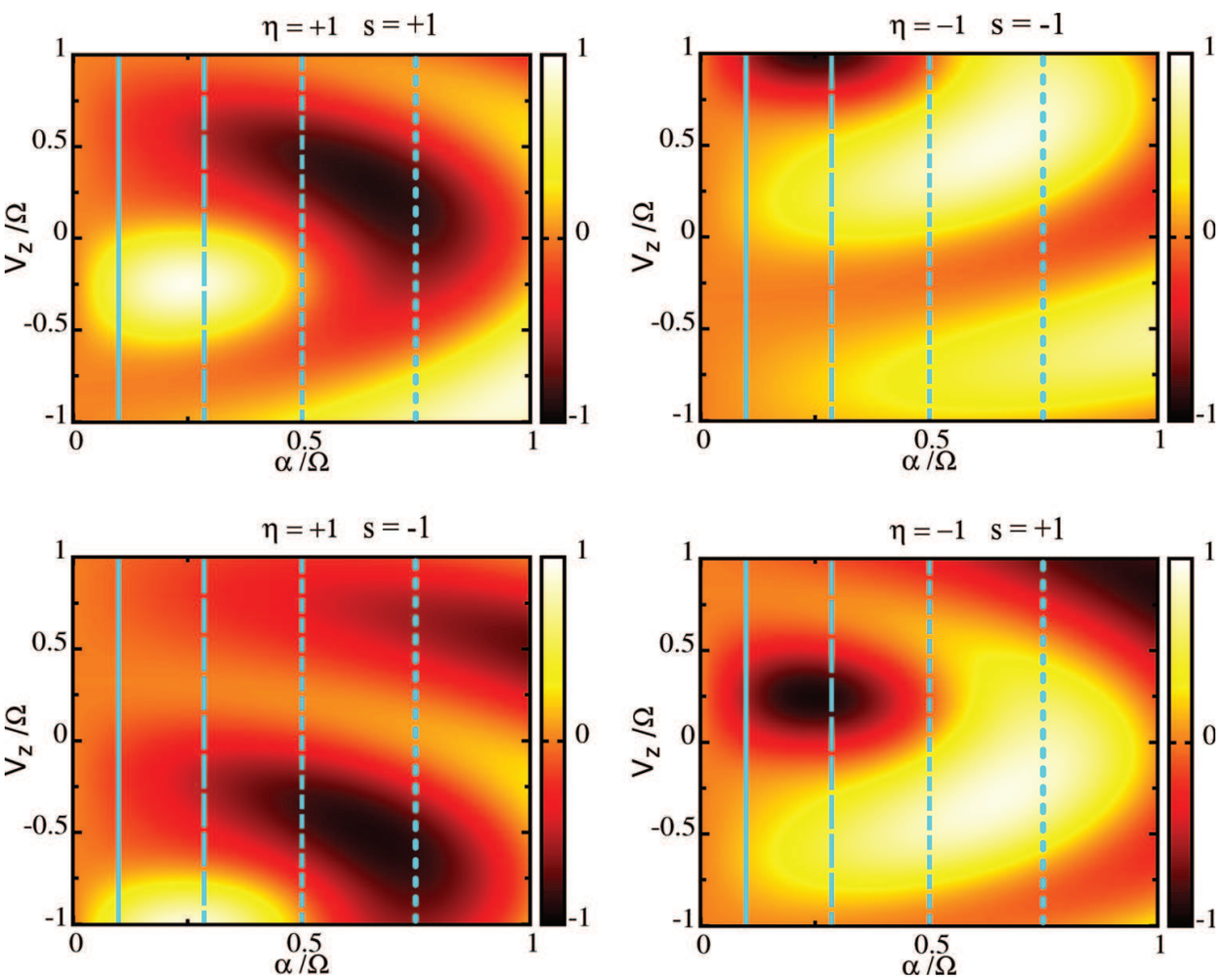

Figure 2. Zero-momentum pseudospin mean polarization for different combinations of the product $s\eta$. The vertical lines correspond to $\alpha = 0.1\Omega$ (continuous), $\alpha = 0.25\Omega$ (large dashed) $\alpha = 0.5\Omega$ (short dashed) and $\alpha = 0.75\Omega$ (large dots), respectively. See discussion in the main text. Adapted from Ref. [35] with permission from APS.

$$\langle \sigma_z \rangle = \alpha \left[\frac{\Delta_s^\eta}{\Gamma^2} \cos\phi (1 - \mathrm{sinc}(2\Gamma T)) - T \sin\phi \mathrm{sinc}^2(\Gamma T) \right]. \tag{73}$$

Setting the value $\phi = \pi/4$, we plot in **Figure 2** the mean pseudospin polarization for the different spin and valley $s\eta$ product combinations.

From this figure, we find that within the low coupling regime ($\alpha \leq 0.1\Omega$), it is in general not possible to induce appreciable changes of the pseudospin polarization and this is related to the fact that the quasi-energy behaviour is essentially controlled by the parameters V_z and λ_{so} which determine the gap behaviour in the static regime. On the other hand, for intermediate ($\alpha = 0.5\Omega$) and large ($\alpha = 0.75\Omega$) values of the coupling to the driving field, that is, beyond the off-resonant condition, effective pseudospin inversion is achievable and therefore a qualitatively different behaviour emerges within this coupling regime.

5. Conclusions

In this chapter, we have described some photoinduced consequences of using periodically driven interactions in graphene-like systems. In essence, these examples provide new insights on the non-trivial behaviour of systems taken out of equilibrium and given the fact that Floquet's theorem allows for a dynamical analysis in terms of an equivalent static description of the physics via the Floquet states, one can infer new physical aspects that can emerge on these systems when subject to such periodic interactions. We consider that these approaches do provide an arena for analysing some interesting phenomena beyond the static limit. The extension of the results presents more involved scenarios, where numerical tools can profit from the simple models described in this chapter and we hope the interested reader could profit from the material presented. One could further explore the dynamical features at finite momentum but refer the reader to Ref. [35] where it is proven that the intermediate light-matter-coupling regime is the physically correct scenario for describing the emergent topological features such as the realization of the single-valley polarized state in silicene. Needless to say that other quantities of interest such as charge and spin currents can be treated within the approximate scenarios discussed in the chapter, they go beyond the main interest of the chapter and are thus not further discussed here.

Appendix

For completeness, in this appendix we include one approximation strategy that can be useful in the semi-analytical treatment of periodically driven systems. This is called the rotating wave approximation concerns with the dynamical evolution of a periodically driven system when the parameters are closed to a resonance. These resonant effects have been shown to be relevant in several experimental situations such as within cavity QED as well as within the context of cold atoms, among others.

Approximate RWA dynamics

In some physical systems, the most important physical effects happen around the first resonance located at around $\omega_0 = \omega$, even a low coupling $\xi = 0.25\omega$. This motivates the search of an analytical solution by means of the rotating wave approximation (RWA) approximation. We now find an approximate analytical solution to the dynamics generated by

$$H(t) = \frac{\omega_0}{2}\sigma_z + A\sin\omega t\sigma_x. \tag{74}$$

Then, in the low coupling regime where the amplitude of the driving field satisfies $\frac{A}{\omega} \ll 1$, we can use the rotating wave approximation (RWA) which amounts to keep those contributions in the driving that are close to resonance, that is, $\omega \sim \omega_0$.

Changing to the interaction representation, the dynamics is dictated by $V_I(t) = e^{i\omega_0 t\sigma_z/2}V(t)$ $e^{-i\omega_0 t\sigma_z/2}$, where $V(t)$ is the time-dependent contribution to Eq. (74). Using the algebra of the Pauli matrices and the explicit time dependence of the driving field, we get

$$V_I(t) = A\sin\omega t(\cos\omega_0 t\sigma_x - \sin\omega_0 t\sigma_y) \tag{75}$$

At this point, we invoke the RWA to get the approximate interaction contribution

$$V_{RWA}(k,t) = i\frac{A}{2}(e^{-i\mu t}\sigma_+ - e^{i\mu t}\sigma_-), \tag{76}$$

where the frequency detuning that characterizes near-resonance contributions is defined as $\mu = \omega - \omega_0$. To get Eq. (76) from Eq. (75), we have assumed $\omega - \omega_0 \sim 0$ and thus have disregarded the quickly oscillating terms proportional to $\omega + \omega_0$ (which are known in the literature as the secular contributions).

Switching back to the Schrödinger representation, we get the total RWA Hamiltonian

$$H_{RWA}(t) = \frac{\omega_0}{2}\sigma_z + ig(e^{-i\omega t}\sigma_+ - e^{i\omega t}\sigma_-), \tag{77}$$

where we have introduced the effective coupling constant $g = \frac{A}{2}$ The Hamiltonian (77) is taking to a time-independent form H_F by means of a periodic unitary transformation $P(t) = e^{-i(\sigma_0+\sigma_z)\omega t/2}$ by means of the standard transformation rule $H_F = P^\dagger(t)H_{RWA}P(t) - iP^\dagger(t)\partial_t P(t)$. Explicitly, we have

$$H_F = -\frac{\omega}{2}\sigma_0 - \frac{\mu}{2}\sigma_z - g\,\sigma_y. \tag{78}$$

Defining the Rabi frequency $\Omega_R = \sqrt{\mu^2 + 4g^2}$, the approximate quasi-energies are found to be given as

$$\varepsilon_\alpha = -\frac{(\omega + \alpha\Omega_R)}{2} \tag{79}$$

where $\alpha = \pm 1$ is the energy subband index. The corresponding approximate Floquet eigenstates are

$$|\Phi_\alpha(k,t)\rangle = \frac{e^{-i\varepsilon_\alpha t}}{\sqrt{2\Omega_R}} \begin{pmatrix} e^{-i\omega t}\sqrt{\Omega_R - \alpha\mu} \\ i\alpha\sqrt{\Omega_R + \alpha\mu} \end{pmatrix}. \tag{80}$$

As before, once the Floquet quasi-energies and eigenstates are found, one can evaluate any physical quantity of interest. For instance, one can evaluate the spin (or any other related quantity that satisfies the Pauli matrices algebra) polarization. In addition, the evaluation of the charge as well as spin currents can be given analytical expressions within the RWA. The relevance of resonant phenomena in nature has already been highlighted in the introduction, but we would like to remember that within this scheme, photon-assisted transport is one of the many resonant processes that can be properly described via the RWA. However, we must mention that one of the drawbacks of the RWA is that it does not take into account a systematic shift of the resonant energies which occurs at higher coupling strengths to the driving field. These are the so-called Bloch-Siegert shifts which emerge from the neglected secular terms. Thus, in order to go to higher coupling strengths and preserve a more realistic physical picture, this secular term should be included. In this context, the Van Vleck quasi-degenerate perturbation theory as well as Magnus expansion approach can be useful semi-analytical tools and we refer the interested reader to Ref. [41] for a detailed treatment of the Magnus expansion approach and to Ref. [42] for a thorough description of the Van Vleck approach.

Author details

Alexander López[1]* and Benjamin Santos[2]

*Address all correspondence to: alexander.lopez@physik.uni-regensburg.de

1 Escuela Superior Politécnica del Litoral, ESPOL, Facultad de Ingeniería Mecánica y Ciencias de la Producción, Campus Gustavo Galindo Km 30.5 Vía Perimetral, Guayaquil, Ecuador

2 INRS-EMT, Université du Québec, Varennes, Québec, Canada

References

[1] Novoselov K. S. et al., Science **306**, 666 (2004).

[2] Novoselov K. S. et al., Nature **438**, 197 (2005).

[3] Geim A. K. and Novoselov K. S., Nat. Mater. **6**, 183 (2007).

[4] Castro Neto A. H. et al., Rev. Mod. Phys. **81**, 109 (2009).

[5] Das Sarma S. et al., Cond-mat.mes-hall, 1003.4701 (2010).

[6] Kane C. L. and Mele E. J., Phys. Rev. Lett. **95**, 226801 (2005), ibid, Phys. Rev. Lett. **95**, 146802 (2005).

[7] Huertas-Hernando D., Guinea F., and Brataas A., Phys. Rev. B **74**, 155426 (2006).

[8] Rashba E., Phys. Rev. B **79**, 161409(R) (2009).

[9] Ertler C. et al., Phys. Rev. B **80**, 041405(R) (2009).

[10] Ando T., Matsumoto Y. and Uemura Y., J. Phys. Soc. Jpn. **39**, 279 (1975).

[11] Klitzing K. v, Dorda G. and Pepper M., Phys. Rev. Lett. **45**, 494 (1980).

[12] Hasan M. Z. and Kane C. L., Rev. Mod. Phys. **82**, 3045 (2010).

[13] Bernevig B. A., Hughes T. L. and Zhang S. C., Science **314**, 1757 (2006).

[14] Fu L., Kane C. L. and Mele E. J., Phys. Rev. Lett. **98**, 106803 (2007).

[15] Goldman N. et al, Phys. Rev. Lett. **105**, 255302 (2010).

[16] Schneider U. et al., Nat. Phys. **8**, 213 (2012).

[17] König M. et al., Science **318**, 766 (2008).

[18] Yang Y. et al, Phys. Rev. Lett. **107**, 066602 (2011)

[19] Lindner N. H., Refael G. and Galinski V., Nat. Phys. **7**, 490 (2011).

[20] Kitagawa T. et al., Phys. Rev. B **82**, 235114 (2010).

[21] Kitagawa T. et al., Phys. Rev. B **84**, 235114 (2011).

[22] Cayssol J., Dóra B., Simon F., and Moessner R., Phys. Status Solidi RRL **7**, 101 (2013).

[23] López A., Di Teodoro A., Schliemann J., Berche B., Santos B., Phys. Rev. B **92**, 235411 (2015).

[24] Grifoni M. and Hänggi P., Phys. Rep. **304**, 229 (1998).

[25] Chu S.-I. and Telnov D. A., Phys. Rep. **390**, 1 (2004).

[26] Shirley J. H. Phys. Rev. **138**, B979 (1965).

[27] Krueckl V. and Kramer T., New J. Phys. **11**, 093010 (2009).

[28] Takeda K. and Shiraishi K., Phys. Rev. B **50**, 14916 (1994).

[29] Guzmán-Verri G. G. and Lew Yan Voon L. C., Phys. Rev. B **76**, 075131 (2007).

[30] Vogt P. et al., Phys. Rev. Lett. **108**, 155501 (2012).

[31] Fleurence A. et al., Phys. Rev. Lett. **108**, 245501 (2012).

[32] Chen L. et al., Phys. Rev. Lett. **109**, 056804 (2012).

[33] Ezawa M., Phys. Rev. Lett. **109**, 055502 (2012).

[34] Ezawa M., Phys. Rev. Lett. **110**, 026603 (2013).

[35] López A., Scholtz A., Schliemann J., and Santos B., Phys. Rev. B **91**, 125105 (2015).

[36] Oka T. and Aoki H., Phys. Rev. B **79**, 081406(R) (2009).

[37] Zhou Y. and Wu M. W., Phys. Rev. B **83**, 245436 (2011).

[38] Calvo H. L., Pastawski H. M., Roche S. and Foa Torres L. E. F., Appl. Phys. Lett. **98**, 232103 (2011).

[39] Lin Q.-g J. Phys. A: Math. Gen. **34**, 1903 (2001).

[40] Liu C. -C., Jiang H. and Yao Y., Phys. Rev. B **84**, 195430 (2011).

[41] Blanes S., Casas F., Oteo J. A. and Ros J., Phys. Rep. **470**, 151 (2009).

[42] Shavitt I. and Redmon L. T., J. Chem. Phys. **73**, 11 (1980).

IntechOpen